Harnessing Chaperones to Generate Small-Molecule Inhibitors of Amyloid ß Aggregation

Jason E. Gestwicki, *et al.*

Science **306**, 865 (2004);
DOI: 10.1126/science.1101262

ization. Rapid changes in the polarity of PIN proteins in response to developmental or environmental cues have been shown to redirect auxin flow and mediate multiple developmental processes (*1*, *3*, *5*), but the mechanism underlying polarity control is largely unresolved. These rapid relocations are enabled by constitutive cycling of PIN proteins. GNOM, an endosomal regulator of vesicle budding that mediates this process, is required for the recycling but does not seem to directly determine the polarity of PIN targeting, because *gnom* mutants show randomized changes in PIN1 polar localization (*15*). In line with this more general function of GNOM in polar auxin transport, most, if not all polar auxin transport–dependent developmental processes are disturbed in *gnom* mutants (*19*). In contrast, the role of PID in controlling PIN polarity is more specific. It appears that PID acts as a binary switch, with subthreshold PID levels leading to basal PIN localization and above-threshold PID levels leading to apical PIN localization. Consistently, the defects observed in both loss- and gain-of-function of *PID* lines can each be ascribed to a reversion in auxin flow. The observation that auxin controls cellular PID levels (*9*) raises the intriguing possibility that PID is involved in a feedback mechanism by which auxin influences the polarity of its own flow. Such a regulatory network has been proposed in the classical "canalization" model to explain the self-organizing properties of vascular tissue differentiation (*20*) and would also account for the dynamic auxin-dependent changes in auxin redistribution underlying phyllotaxis (*3*, *18*). Even though endogenous PID acts in a limited subset of PIN-dependent development processes, many more cells are competent to respond to PID overexpression. In *Arabidopsis*, PID belongs to a family of 23 protein kinases, the members of which are differentially expressed. It is therefore likely that ectopic PID expression reveals functions that are normally represented by these different PID family members. Although further experimentation is needed to determine whether PIN proteins are direct targets of PID, it is clear that PID-dependent phosphorylation is an essential intermediate step in the control of polar PIN protein targeting, and thus of directional auxin flow regulating patterning processes.

References and Notes

1. J. Friml *et al.*, *Nature* **426**, 147 (2003).
2. J. Mattsson, W. Ckurshumova, T. Berleth, *Plant Physiol.* **131**, 1327 (2003).
3. E. Benkova *et al.*, *Cell* **115**, 591 (2003).
4. J. Friml, K. Palme, *Plant Mol. Biol.* **49**, 273 (2002).
5. J. Friml, J. Wisniewska, E. Benkova, K. Mendgen, K. Palme, *Nature* **415**, 806 (2002).
6. N. Geldner *et al.*, *Cell* **112**, 219 (2003).
7. S. R. M. Bennett, J. Alvarez, G. Bossinger, D. R. Smyth, *Plant J.* **8**, 505 (1995).
8. S. K. Christensen, N. Dagenais, J. Chory, D. Weigel, *Cell* **100**, 469 (2000).
9. R. Benjamins, A. Quint, D. Weijers, P. Hooykaas, R. Offringa, *Development* **128**, 4057 (2001).
10. A. Muller *et al.*, *EMBO J.* **17**, 6903 (1998).
11. J. Friml *et al.*, *Cell* **108**, 661 (2002).
12. I. Ottenschlager *et al.*, *Proc. Natl. Acad. Sci. U.S.A.* **100**, 2987 (2003).
13. J. Friml *et al.*, data not shown.
14. K. Ljung *et al.*, *Plant Mol. Biol.* **50**, 309 (2002).
15. T. Steinmann *et al.*, *Science* **286**, 316 (1999).
16. D. Weijers, N. Geldner, R. Offringa, G. Jurgens, *Nature* **414**, 709 (2001).
17. D. Weijers *et al.*, *Development* **128**, 4289 (2001).
18. D. Reinhardt *et al.*, *Nature* **426**, 255 (2003).
19. N. Geldner *et al.*, *Development* **131**, 389 (2004).
20. T. Berleth, T. Sachs, *Curr. Opin. Plant Biol.* **4**, 57 (2001).
21. Materials and methods are available as supporting material on *Science* Online.

22. We thank the Nottingham *Arabidopsis* stock center for providing *eir1-1*, S. Christensen for the *35S::MPID* line, C. Luschnig for the antibody to PIN2, L. Gälweiler for help with PIN localization studies, A. Vivian-Smith for helpful discussions, G. Lamers for help with microscopy, and P. Hock for art work. This work was supported by the Volkswagen Stiftung program (J.F. and M.M.), the Deutsche Forschungsgemeinschaft (grants SFB592 and SPP1108 to O.T. and K.P.), the Research Council for Earth and Life Sciences (ALW) with financial aid from the Dutch Organization of Scientific Research (NWO) (D.W.) by the European Union 5th Framework Project QLG2-CT-2001-01453 CerealGene Tags (P.B.F.O.), and by the Swedish Research Council (K.L. and G.S.). X.Y. was supported by a Leiden–Peking University exchange grant.

Supporting Online Material

www.sciencemag.org/cgi/content/full/306/5697/862/DC1
Materials and Methods
Figs. S1 to S3
References

24 May 2004; accepted 9 September 2004

Harnessing Chaperones to Generate Small-Molecule Inhibitors of Amyloid β Aggregation

Jason E. Gestwicki, Gerald R. Crabtree, Isabella A. Graef*

Protein aggregation is involved in the pathogenesis of neurodegenerative diseases and hence is considered an attractive target for therapeutic intervention. However, protein-protein interactions are exceedingly difficult to inhibit. Small molecules lack sufficient steric bulk to prevent interactions between large peptide surfaces. To yield potent inhibitors of β-amyloid (Aβ) aggregation, we synthesized small molecules that increase their steric bulk by binding to chaperones but also have a moiety available for interaction with Aβ. This strategy yields potent inhibitors of Aβ aggregation and could lead to therapeutics for Alzheimer's disease and other forms of neurodegeneration.

Aggregation of Aβ peptide, generated by proteolytic cleavage of amyloid precursor protein (APP), is a key event in the pathogenesis of Alzheimer's disease (*1*–*3*). Genetic studies on Alzheimer's disease implicate mutations in APP and in genes involved in APP processing (*4*) in disease development. Because genetic factors that contribute to Alzheimer's disease also promote Aβ aggregation, inhibition of polymerization may have therapeutic benefit. However, this process has proven extremely difficult to prevent (*5*, *6*). One hurdle to overcome is the poor capacity of low molecular weight drugs to interfere with the protein-protein interactions that generate toxic Aβ aggregates. Blocking protein-protein interactions is a general problem and, despite the importance of these interactions in biologic processes, few inhibitors have been identified (*7*, *8*). The binding energy that drives protein-protein contacts is typically distributed over a large area and, unlike enzymes, these surfaces lack a defined "hotspot" for pharmacological intervention. Additionally, protein surfaces possess a high level of plasticity that can serve to accommodate small molecules, thereby avoiding inhibition.

To approach this problem, we envisioned a Trojan Horse strategy in which a small bifunctional molecule would gain access to the relevant biologic compartment, bind tightly to a chaperone, and thereby gain the steric bulk needed to disrupt a protein-protein interaction (Fig. 1A). Chaperones are ideally suited for this approach, as they bind folding or misfolded proteins via exposed hydrophobic surfaces.

In this strategy, one end of the bifunctional molecule binds the FK506 binding protein (FKBP) chaperone family of peptidyl prolyl cis-trans isomerases. FKBPs are encoded by 23 different genes, are highly expressed in all mammalian cells (*9*, *10*), and are good candidates for recruitment by bifunctional molecules (*11*–*15*). The other end

Department of Pathology, Howard Hughes Medical Institute, Stanford University Medical School, Stanford, CA 94305, USA.

*To whom correspondence should be addressed. E-mail: graef@cmgm.stanford.edu

of the bifunctional molecule is free to interact with aggregating Aβ. A number of organic compounds, including Congo Red (CR), function as amyloid ligands. These compounds are unsuitable for therapeutic use because high molar ratios of drug to Aβ are required to inhibit aggregation (*5*, *6*). To investigate whether chaperone recruitment could empower these ineffective small molecules with the ability to interfere with Aβ aggregation and toxicity, we synthesized SLF-CR (Fig. 1B) (fig. S1), which is composed of CR covalently tethered to a synthetic ligand for FKBP (SLF) (*16*).

To assess the impact of chaperone recruitment on the potency of aggregation inhibitors, we incubated Aβ(1-42) in the presence of drug and FKBP. Fibrillogenesis was followed in real time by turbidity measurements. SLF-CR/FKBP (10 μM) completely blocked the formation of Aβ aggregates capable of scattering light (Fig. 1C). Even at nanomolar concentrations, SLF-CR/FKBP [median inhibitory concentration (IC_{50}) = 0.43 μM] delayed amyloid aggregation (Fig. 1D). Inhibition by SLF-CR required FKBP, but the chaperone alone did not change Aβ aggregation. In contrast, CR was a modest inhibitor of turbidity and FKBP did not alter its potency.

As a second measure of inhibition, we explored the aggregation of Aβ by the thioflavin T assay. Thioflavin T fluorescence increases in the presence of Aβ aggregates, which makes this an attractive assay for screening inhibitors (*17*). The IC_{50} of SLF-CR/FKBP for decreasing the concentration of thioflavin T–binding species was lower than that of CR/FKBP by a factor of about 5 (Fig. 1E). Increasing the molar equivalents of FKBP further enhanced the potency of SLF-CR (Fig. 1F). In the absence of FKBP, SLF-CR and CR had similar activity. These results suggest that drug-mediated recruitment of FKBP is required for enhanced potency.

Recent evidence has suggested a role for nonfibrillar Aβ aggregates in the pathology of Alzheimer's disease (*1*–*3*). Preventing formation of these intermediates is therefore an important measure of inhibitory potency (*2*, *18*). To explore the ultrastructure of Aβ aggregates, we examined drug-treated mixtures by transmission electron microscopy (TEM) and atomic force microscopy (AFM) (*19*). At a concentration of 1 μM, CR, SLF-CR, and CR/FKBP were ineffective at reducing the size and abundance of Aβ fibrils (Fig. 2, A and B). However, consistent with the thioflavin T and turbidity experiments, SLF-CR/FKBP almost fully blocked fibril formation. By AFM, smaller, less elongated species were observed in samples treated with SLF-CR/FKBP; these probably represent an intermediate trapped before the formation of fibrils. The particles were approximately uniform in size (28 ± 5 nm^2; N = 50), which suggested that SLF-CR/FKBP interrupted fibril formation at a discrete step in the aggregation pathway. Because these species were not observed in samples treated with CR/FKBP, they might represent a qualitative difference between the mechanisms of action of CR and SLF-CR/FKBP. Furthermore, electrophoretic analysis of Aβ oligomers showed a predominance of small aggregates in Aβ samples treated with SLF-CR/FKBP but not CR/FKBP (fig. S2B).

Although a strategy that interrupts the aggregation process provides mechanistic insight, the most important criterion of therapeutic potential is the capacity to prevent the formation of neurotoxic aggregates. We examined whether the bifunctional drugs could inhibit neurotoxicity of in vitro aggregated Aβ. The cell viability of P0 hippocampal neurons was assessed with the 3-(4,5-dimethyl-2-thiazoyl)-2,5-diphenyltetrazoliumbromide (MTT) assay (Fig. 3A). SLF-CR/FKBP-treated Aβ samples were substantially less toxic than untreated or CR/FKBP-treated samples (Fig. 4A). The EC_{50} of SLF-CR/FKBP was lower than that of CR/FKBP by a factor of about 4 (0.9 ± 1.3 μM and 4.2 ± 1.4 μM, respectively). SLF-CR's ability to prevent Aβ-induced neuronal death was dependent on the concentration of FKBP (Fig. 3B). Thus, drug-mediated recruitment of FKBP not only blocked aggregation but could also inhibit Aβ toxicity.

To examine the morphology of the treated neurons, we applied Aβ and drug-protein combinations to cultured hippocampal neurons.

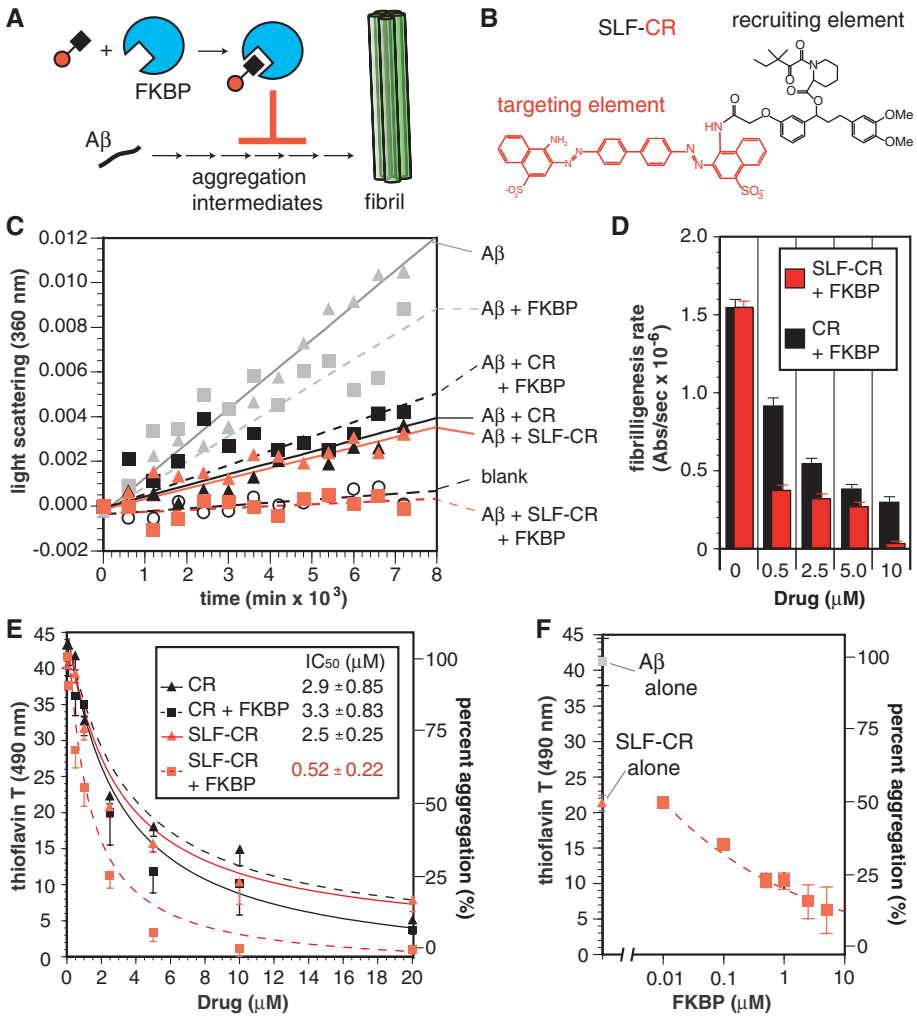

Fig. 1. The combination of SLF-CR and FKBP inhibits aggregation of Aβ(1-42). **(A)** Model of Aβ fibrillogenesis and interruption by a bifunctional small molecule recruiting FKBP to increase the drug's steric bulk. **(B)** The chemical structure of SLF-CR is shown with the targeting domain, CR, in red and the recruiting domain, SLF, in black. **(C)** Inhibition of Aβ fibrillogenesis as measured by light scattering. Drug was added to a concentration of 10 μM, FKBP to 1 μM, and Aβ to 25 μM. **(D)** The initial rate of turbidity as a function of drug concentration was assumed to be linear, which yielded the fibrillogenesis rate. **(E)** Inhibition of Aβ fibrillogenesis as measured by thioflavin T fluorescence. Results are averages (±SEM) of at least three independent experiments performed in duplicate. **(F)** Impact of FKBP availability on inhibition of thioflavin T reactivity mediated by 2.5 μM SLF-CR. Results are averages (±SEM) of two experiments performed in triplicate.

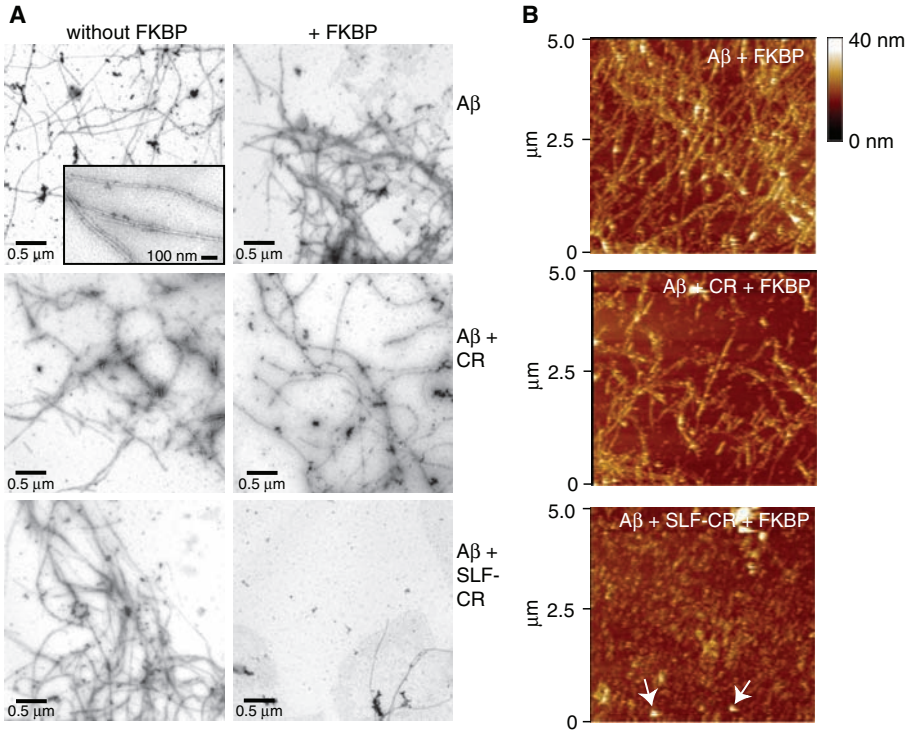

Fig. 2. Direct visual investigation of Aβ(1-42) fibrils. (**A**) TEM images depict the ultrastructure and distribution of amyloid fibrils. Images are representative of at least three independent experiments. The inset shows fibrils in greater detail. Fibrils in samples treated with SLF-CR and FKBP were uncommon, but one is shown in the figure to illustrate the similarity to those in other samples. (**B**) Representative AFM images show Aβ treated with FKBP alone, CR/FKBP, or SLF-CR/FKBP. The *x*-*y* distances are shown at the left; color scale at right indicates height (*z* direction). An arrow indicates the position of species common to samples treated with SLF-CR/FKBP.

Cell death was measured by terminal deoxynucleotidyl transferase–mediated deoxyuridine triphosphate nick end labeling (TUNEL) assay, and cell morphology was assessed with a cytoskeletal immunostain. As expected, treatment with Aβ induced cell death as well as abnormal cell morphology (Fig. 3C) (fig. S3); neurites became dystrophic, some neurons detached from the slides, and those remaining showed signs of nuclear fragmentation and membrane blebbing. Incubation of Aβ with FKBP, CR, CR/FKBP, or SLF-CR failed to reduce the number of TUNEL-positive cells or prevent changes in cell morphology. The SLF-CR/FKBP combination, however, markedly blocked toxicity. Moreover, SLF-CR/FKBP–treated neurons displayed mostly normal morphology (Fig. 3C). These studies show that FKBP recruitment can protect cultured neurons from cell death triggered by toxic Aβ aggregates.

Our strategy is designed to allow bifunctional drugs to wield the steric bulk of FKBP and prevent Aβ from joining the nascent fibril. Improved coverage of the Aβ surface might provide superior inhibition, possibly by altering the orientation of FKBP relative to the Aβ surface. Our synthetic strategy permits the assembly of bifunctional compounds from a collection of modular targeting domains, recruiting domains, and interchangeable linkers. Therefore, we envisioned that by installing linkers that vary in length and flexibility, we might identify compounds that

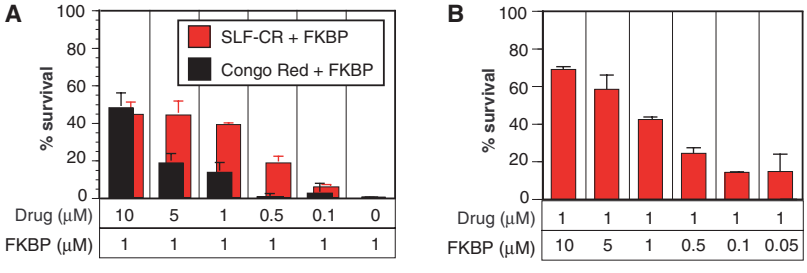

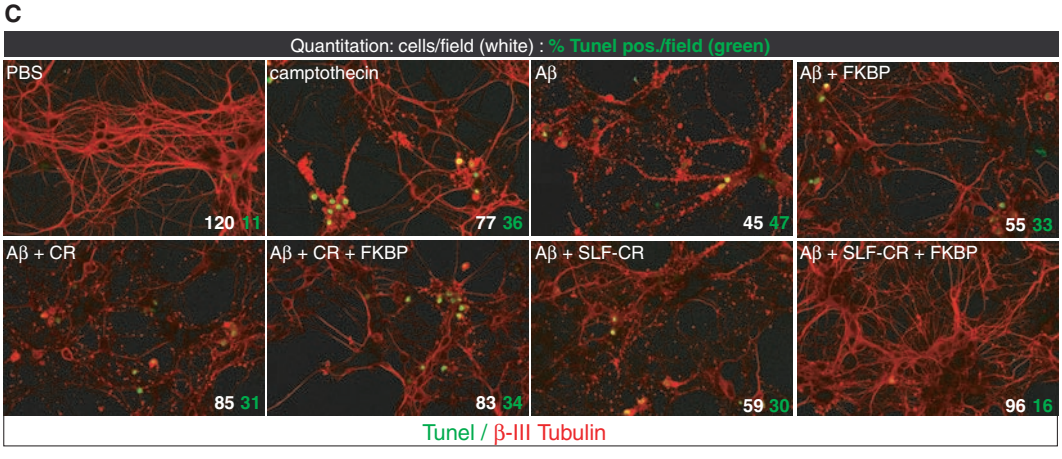

Fig. 3. The combination of SLF-CR and FKBP reduces the toxicity of Aβ(1-42). (**A**) Cell viability of hippocampal neurons as measured by the conversion of MTT. Results are averages (±SEM) of at least two experiments performed in triplicate. At the concentrations used, neither the compounds (up to 20 μM) nor FKBP (1 μM) were toxic in the absence of Aβ (fig. S2C). (**B**) Dependence of cell viability on the concentration of FKBP. In these experiments, Aβ(1-42) (100 μM) was treated with varying levels of FKBP at constant drug concentrations (1 μM). Results are averages (±SEM) of two experiments performed in triplicate. (**C**) The viability and morphology of hippocampal neurons were determined by labeling with TUNEL (green) and antibody to β-III tubulin (red). In the lower right corner of each panel, the total number of cells per 40× field (white) and percent TUNEL-positive cells in the same fields (green) are shown (n = 200 to 600 cells). Cells treated with phosphate-buffered saline (PBS) or the toxin camptothecin (0.6 mg/ml) are shown for comparison.

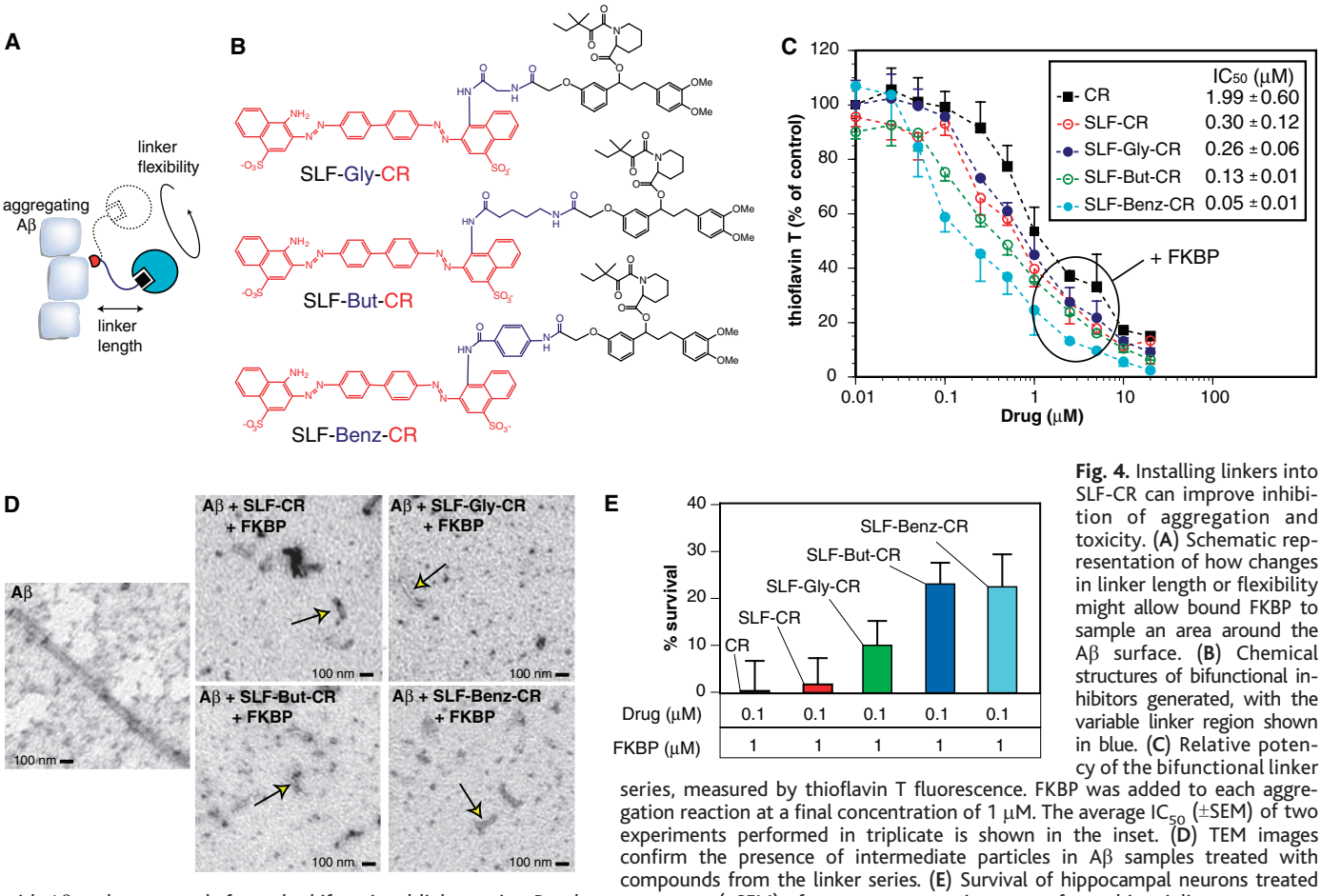

Fig. 4. Installing linkers into SLF-CR can improve inhibition of aggregation and toxicity. (**A**) Schematic representation of how changes in linker length or flexibility might allow bound FKBP to sample an area around the Aβ surface. (**B**) Chemical structures of bifunctional inhibitors generated, with the variable linker region shown in blue. (**C**) Relative potency of the bifunctional linker series, measured by thioflavin T fluorescence. FKBP was added to each aggregation reaction at a final concentration of 1 μM. The average IC_{50} (±SEM) of two experiments performed in triplicate is shown in the inset. (**D**) TEM images confirm the presence of intermediate particles in Aβ samples treated with compounds from the linker series. (**E**) Survival of hippocampal neurons treated with Aβ and compounds from the bifunctional linker series. Results are averages (±SEM) of one or two experiments performed in triplicate.

permit FKBP to scan the Aβ surface for favorable arrangements (Fig. 4A).

In a search for more potent inhibitors, we generated a series of bifunctional compounds that vary in the linker (Fig. 4B) (fig. S3A). These molecules were named according to the reagent used to create the linker (i.e., the amino acid glycine was used to generate SLF-Gly-CR). When we tested these compounds in conjunction with FKBP in the thioflavin T assay, we found that SLF-But-CR/FKBP and SLF-Benz-CR/FKBP were potent inhibitors (Fig. 4C) (fig. S3B). The most active compound, SLF-Benz-CR/FKBP, had an IC_{50} of about 50 nM, which is lower than that of CR by a factor of 40 and represents an improvement over the parent combination, SLF-CR/FKBP, by a factor of 6. Like SLF-CR, the potency of the compounds was dependent on the availability of FKBP (fig. S3B). TEM revealed that the size and shape of Aβ intermediates were similar in samples treated with each of the bifunctional molecules (Fig. 4D). Thus, regardless of the properties of the linker, a common FKBP-drug-Aβ complex formed.

To explore the role of the linker in reduction of Aβ toxicity, we measured neuronal viability. Consistent with the rank order as measured by thioflavin T fluorescence, SLF-Benz-CR/FKBP and SLF-But-CR/FKBP were, at nanomolar concentrations, significantly more potent than CR/FKBP or SLF-CR/FKBP (Fig. 4E) (fig. S3C). Even at the high molar concentrations of Aβ used in these experiments, SLF-Benz-CR remained active at 100 nM. Despite the modest number of compounds in the linker series, potent inhibitors could be uncovered by assembling modular components.

Our results indicate that recruitment of chaperones can block Aβ fibril formation and substantially reduce Aβ toxicity. Whereas other inhibitors of Aβ aggregation, such as CR and short peptides, are active in the 2 to 10 μM range (*5*, *6*), our best compound was effective at 50 nM. This improvement is likely a result of the inhibitory mechanism used, because the bifunctional molecules were not superior to CR in the absence of chaperone. Analogs based on the SLF-CR model may have potential as therapeutics for Alzheimer's disease. The advantage of therapeutic intervention at the aggregation step is that it targets a purely pathological event in disease development. Thus, directly inhibiting Aβ aggregation with the recruited-chaperone approach might provide a viable complement to recent efforts to reduce the rate of Aβ release (*20*, *21*), enhance its clearance (*22*, *23*), or template nontoxic aggregates (*24*–*26*).

References and Notes

1. J. Hardy, D. J. Selkoe, *Science* **297**, 353 (2002).
2. W. L. Klein, *Neurochem. Int.* **41**, 345 (2002).
3. J. D. Harper, S. S. Wong, C. M. Lieber, P. T. Lansbury Jr., *Biochemistry* **38**, 8972 (1999).
4. D. J. Selkoe, M. B. Podlisny, *Annu. Rev. Genomics Hum. Genet.* **3**, 67 (2002).
5. V. M.-Y. Lee, *Neurobiol. Aging* **23**, 1039 (2002).
6. M. A. Findeis, *Biochim. Biophys. Acta* **1502**, 76 (2000).
7. A. V. Veselovsky *et al.*, *J. Mol. Recognit.* **15**, 405 (2002).
8. W. L. Delano, M. H. Ultsch, A. A. De Vos, J. A. Wells, *Science* **287**, 1279 (2000).
9. A. Galat, *Curr. Top. Med. Chem.* **3**, 1315 (2003).
10. R. F. Standaert, A. Galat, G. L. Verdine, S. L. Schreiber, *Nature* **346**, 671 (1990).
11. R. Briesewitz, G. T. Ray, T. J. Wandless, G. R. Crabtree, *Proc. Natl. Acad. Sci. U.S.A.* **96**, 1953 (1999).
12. D. M. Spencer, T. J. Wandless, S. L. Schrieber, G. R. Crabtree, *Science* **262**, 1019 (1993).
13. K. Stankunas *et al.*, *Mol. Cell* **12**, 1615 (2003).
14. P. D. Braun *et al.*, *J. Am. Chem. Soc.* **125**, 7575 (2003).
15. R. Pollock, M. Giel, K. Linher, T. Clackson, *Nature Biotechnol.* **20**, 729 (2002).
16. D. A. Holt *et al.*, *J. Am. Chem. Soc.* **115**, 9925 (1993).
17. H. LeVine III, *Methods Enzymol.* **309**, 274 (1999).
18. E. H. Koo, P. T. Lansbury Jr., J. W. Kelly, *Proc. Natl. Acad. Sci. U.S.A.* **96**, 9989 (1999).
19. S. S. Wong, J. D. Harper, P. T. Lansbury Jr., C. M. Lieber, *J. Am. Chem. Soc.* **120**, 603 (1998).
20. M. Citron, *Neurobiol. Aging* **23**, 1017 (2002).
21. M. L. Michaelis, *J. Pharmacol. Exp. Ther.* **304**, 897 (2003).

22. C. Janus, M. A. Chishti, D. Westway, *Biochim. Biophys. Acta* **1502**, 63 (2000).
23. R. Kayed *et al.*, *Science* **300**, 486 (2003).
24. J. Ghanta, C.-L. Shen, L. L. Kiessling, R. M. Murphy, *J. Biol. Chem.* **271**, 29525 (1996).
25. J. C. Sacchettini, J. W. Kelly, *Nature Rev. Drug Discov.* **1**, 267 (2002).
26. F. E. Cohen, J. W. Kelly, *Nature* **426**, 905 (2003).
27. This work is dedicated to A. Graef. We thank Y.-M. Lin and T. Wandless for starting materials; V. Devasthali for experimental support; and L. Mucke, C. Cairo, T. Buchholz, and Crabtree laboratory members for helpful discussions. Supported by National Institute of Neurological Disorders and Stroke grant NS046789 and by an award from the Christopher Reeve Paralysis Foundation. J.E.G. is a Helen Hay Whitney postdoctoral fellow. G.R.C. is an Investigator of the Howard Hughes Medical Institute.

Supporting Online Material
www.sciencemag.org/cgi/content/full/306/5697/865/DC1
Materials and Methods
SOM Text
Figs. S1 to S3
References

8 June 2004; accepted 3 September 2004

Ciliary Photoreceptors with a Vertebrate-Type Opsin in an Invertebrate Brain

Detlev Arendt,[1]*† Kristin Tessmar-Raible,[2]*‡ Heidi Snyman,[1] Adriaan W. Dorresteijn,[3] Joachim Wittbrodt[1]†

For vision, insect and vertebrate eyes use rhabdomeric and ciliary photoreceptor cells, respectively. These cells show distinct architecture and transduce the light signal by different phototransductory cascades. In the marine ragworm *Platynereis*, we find both cell types: rhabdomeric photoreceptor cells in the eyes and ciliary photoreceptor cells in the brain. The latter use a photopigment closely related to vertebrate rod and cone opsins. Comparative analysis indicates that both types of photoreceptors, with distinct opsins, coexisted in Urbilateria, the last common ancestor of insects and vertebrates, and sheds new light on vertebrate eye evolution.

In animal photoreceptor cells (PRCs), the surface membrane is enlarged for the storage of opsin photopigment (*1*). Two major types of PRCs are recognized by electron microscopy (table S1). In rhabdomeric PRCs, the apical cell surface folds into microvilli. This is the predominant type of PRC used for vision in invertebrates. In contrast, in vertebrates, the rods and cones of the retina and the PRCs of the pineal eye, a light-sensitive structure in the dorsal diencephalon, are of the ciliary type. In ciliary PRCs, the membrane of the cilium is folded for surface enlargement. To elucidate the evolution of ciliary PRCs, we investigated the photosensitive system in *Platynereis dumerilii* (Polychaeta, Annelida, Lophotrochozoa) (*2*, *3*). This species shows ancestral anatomy and development and an ancestral gene inventory (*2*, *4*). In addition, polychaetes and vertebrates are evolutionarily far apart (*2*), and thus any feature specifically shared between them as a result of their common evolutionary heritage necessarily existed in Urbilateria, the last common ancestor of all animals with bilateral symmetry.

Platynereis develops different pairs of eyes (*5*), as demarcated by opsin expression in Fig. 1A: "larval eyes," implicated in larval phototaxis, and "adult eyes," active in adult vision. All these eyes use rhabdomeric PRCs. The two pairs of adult eyes originate from a single anlage that is not yet split at the stage of the analysis. To identify ciliary PRCs, we used an antibody directed against acetylated α-tubulin (Fig. 1A) (*3*), which specifically labels stabilized microtubules in cilia and axons. In addition to the axonal scaffold, we detected two paired structures in the developing median brain, on the dorsal side of the apical organ (Fig. 1A, arrows). Electron microscopy (*3*) revealed that these structures represent multiple cilia (Fig. 1, B to E) that branch out into digits, each inheriting one of the peripheral microtubule doublets (Fig. 1, C and D). Such ciliated cells have been described for the brain of adult nereidids (*6*) and other polychaetes (*7*) and nemertines (*8*),

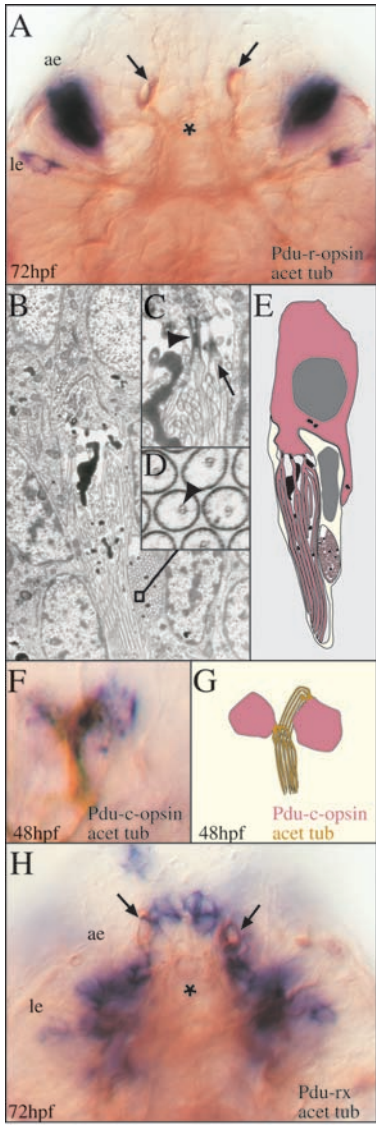

Fig. 1. *Pdu-c-opsin* and *Pdu-rx* expression in *Platynereis* ciliary photoreceptors (cPRCs). (A, F, H) Apical views of in situ hybridizations (blue) double-stained with an antibody to acetylated tubulin (brown). (**A**) *Pdu-r-opsin* expression (blue) 72 hours after fertilization (72 hpf), localized to larval and adult eyes (le, ae). (**B**) Electron micrograph of brain cPRCs. (**C**) Basal bodies of cilia (arrowhead), ramification in longitudinal section (arrow). (**D**) Ramifications in cross section with one doublet of microtubules (arrowhead). (**E**) Schematic based on (B). (**F**) *Pdu-c-opsin* expression (blue) in cPRCs (brown) at 48 hpf. (**G**) Schematic of (F). (**H**) Brain cPRCs (arrows) show high expression of *Pdu-rx*. Asterisks demarcate the apical organ. Magnification [(A) and (H)] ×300, (B) ×3000, (C) ×3800, (D) ×25,000, and (F) ×1200.

[1]Developmental Biology Department, European Molecular Biology Laboratory, Meyerhofstrasse 1, 69012 Heidelberg, Germany. [2]Philipps-Universität Marburg, Institut für Spezielle Zoologie, Karl-von-Frisch-Strasse 8, 35032 Marburg, Germany. [3]Justus-Liebig-Universität Giessen, Institut für Allgemeine und Spezielle Zoologie, Stephanstrasse 24, 35390 Giessen, Germany.

*These authors contributed equally to this work.
†To whom correspondence should be addressed. E-mail: detlev.arendt@embl.de (D.A.), jochen.wittbrodt@embl.de (J.W.)
‡Present address: European Molecular Biology Laboratory, Meyerhofstrasse 1, 69012 Heidelberg, Germany.